#410250

PHYSICAL PROPERTY CHARACTERIZATION OF MISCELLANEOUS ROCK SAMPLES CONTRACT AA-2896

Submitted to:

SANDIA NATIONAL LABORATORIES
MS 1324
P.O. Box 5800
Albuquerque, NM 87185-1324

Attn: Dr. Richard L. Beauheim

TR97-03
August, 1996

TerraTek

TerraTek, Inc.
University Research Park
400 Wakara Way
Salt Lake City, Utah 84108 U.S.A.

PHYSICAL PROPERTY CHARACTERIZATION OF MISCELLANEOUS ROCK SAMPLES CONTRACT AA-2896

Submitted to:

SANDIA NATIONAL LABORATORIES
MS 1324
P.O. Box 5800
Albuquerque, NM 87185-1324

Attn: Dr. Richard L. Beauheim

Submitted by:

TerraTek, Inc.
University Research Park
420 Wakara Way
Salt Lake City, Utah 84108

TR97-03
August, 1996

Table of Contents

List of Tables

List of Figures

1 INTRODUCTION

Cores were supplied by Sandia National Laboratory (SNL) for rock characterization testing in support for the Waste Isolation Pilot Plant (WIPP). The WIPP is the U.S. Department of Energy's planned repository for transuranic waste generated by defense programs. Hence, evaluation of transport properties of surrounding rock formations is critical for accurate assessment of the long-term performance of the repository. The laboratory tests were designed to provide information on transport properties for rock units in the vicinity of the WIPP site. The test program consisted of:

1) Effective Porosity Measurements;
2) Single Phase Gas Permeability Measurements - (determined in two directions);
3) Single Phase Liquid Permeability Measurements (in one direction);
4) Determination of Formation Factor; and,
5) Pore Volume Compressibility Measurements.

Cores sent by SNL were from six distinct zones/formations designated as Culebra, Magenta, Dewey Lake, Forty-Niner, Tamarisk, and Unnamed Lower Member. The Culebra is predominantly characterized as a poorly consolidated, argillaceous dolomite. The Magenta consists of more competent, fine-grained dolomite/mudstone. The Dewey Lake consists of competent sandstones and siltstones. Finally, the Forty-Niner, Tamarisk and Unnamed Lower Member contain anhydrite and claystone intervals. Detailed lithologic and mineralogic characterization was not performed by TerraTek on this core material. Recognizing limited quantities of core and sample-to-sample heterogeneity, and to obtain the maximum amount of information from a given test sample, multiple tests were typically conducted on the same test plug. The testing matrix for this program is summarized in Table 1.

2 Core Receipt and Inspection

Two pallets each containing seven core boxes were received at TerraTek on July 17, 1995. The core containers were immediately inspected for transportation damage and logged-in using the designated Quality Assurance Program Plan (QAPP) worksheet (Worksheet No. 1). Following the initial evaluation of the core containers, each core box was opened and its contents were inspected. Pertinent information consisting of core depths, dimensions, and general condition, were noted on Worksheet No. 1. A summary of the initial core inspection is provided in Table 2. In general, the Culebra core was loosely sealed in Pro-Tec Core foil wrapping, while all other

core material was sealed in zip-lock bags. Core conditions ranged from good to poor, with many core sections exhibiting fractures, broken pieces, and irregular whole core diameters.

Table 1: Summary of Test Program - Matrix

Formation	Depth Range (ft)	Total Number of Samples	Tests					
			Porosity	K_{Vgas}	K_{Hgas}	$K_{Hliquid}$	F_R	PVC
Culebra	740-760	44	24	24	20	-	21	-
Magenta	622-645	9	9	5	4	-	-	4
Dewey Lake	123-563	16	8	8	8	-	-	-
Forty-Niner	567-622	14	14	7	7	3	-	7
Tamarisk	664-732	14	14	7	7	2	-	7
Un-named Lower Member	762-780	6	6	3	3	2	-	3
Totals		103	75	54	49	7	21	21

K_{Vgas} = single-phase gas permeability - vertical direction (along core axis).
K_{Hgas} = single-phase gas permeability - horizontal direction (normal to core axis).
$K_{Hliquid}$ = single-phase liquid permeability - horizontal direction (normal to core axis).
F_R = resistivity formation factor.
PVC = pore volume compressibility.

Table 2: Initial Core Conditions

Box ID	Shipping ID	Formation/ Unit	Depth (ft)	Whole Core Diameter (in)	Conditions/Comments
1/7	Pallet 1 RC-1	Culebra	740.5-742.9	3.25	Whole core in poor condition - samples broken in many pieces with the longest piece = 4 inches. Core shipped in Pro-Tec Core foil.
2/7	Pallet 1 RC-2	Culebra	742.9-745.5	3.25	Whole core in poor condition - samples broken in many pieces with the longest piece = 7 inches. Core shipped in Pro-Tec Core foil.
3/7	Pallet 1 RC-3	Culebra	745.5-748.2	3.25	Whole core in fair condition - samples broken in multiple pieces with the longest piece = 10 inches. Core shipped in Pro-Tec Core foil.
4/7	Pallet 1 RC-4	Culebra	748.2-750.5	3.25	Whole core in poor condition - samples broken in many pieces with the longest piece = 3 inches. Core shipped in Pro-Tec Core foil.
5/7	Pallet 1 RC-5	Culebra	755.5-758.0	3.25	Whole core in poor condition - samples broken in many pieces with the longest piece = 2.5 inches. Core shipped in Pro-Tec Core foil.
6/7	Pallet 1 RC-6	Culebra	758.0-760.5	3.25	Whole core in fair condition - samples broken in multiple pieces with the longest piece = 9.5 inches. Core shipped in Pro-Tec Core foil.
7/7	Pallet 1 M-2	Unnamed Lower Member	762.3-763.1	3.25	Whole core in fair condition - core is in two pieces, 3 and 5 inches long. Core shipped in zip-lock bag.
7/7	Pallet 1 M-2 Lower	Unnamed Lower Member	770.1-770.7	3.25	Whole core in fair to poor condition - core is in two pieces, 3 and 2.75 inches long. Irregular core diameter. Core shipped in zip-lock bag.
7/7	Pallet 1 A-1	Unnamed Lower Member	772.9-773.7	3.25	Whole core in good condition. Single piece 9 inches long shipped in zip-lock bag.
7/7	Pallet 1 A-1 Middle	Unnamed Lower Member	779.0-779.5	3.25	Whole core in poor condition. Fractured into several pieces with largest piece 1.75 inches long. Core shipped in zip-lock bag.

Table 2: Initial Core Conditions - continued

Box ID	Shipping ID	Formation/ Unit	Depth (ft)	Whole Core Diameter (in)	Conditions/Comments
1/7	Pallet 2 A-3 Top	Tamarisk	664.6-665.1	3.25	Whole core in good condition - one piece 6 inches in length. Core shipped in zip-lock bag.
1/7	Pallet 2 A-2	Tamarisk	724.0-724.7	3.25	Whole core in good condition - one piece 8.75 inches in length. Core shipped in zip-lock bag.
2/7	Pallet 2 M-3	Tamarisk	712.9-713.3	3.25	Whole core in fair condition - core broken in two pieces, 2.5 and 4.5 inches in length. Core has irregular diameter. Core shipped in zip-lock bag.
2/7	Pallet 2 DL-NH	Dewey Lake	562.4-563.0	3.25	Whole core in good condition - one piece 7 inches in length. Core shipped in zip-lock bag.
2/7	Pallet 2 M-3	Tamarisk	720.9-721.5	3.25	Whole core in fair condition - core broken in two pieces, 2.75 and 3.5 inches in length. Core has irregular diameter. Core shipped in zip-lock bag.
3/7	Pallet 2 M-4 Base	Forty-Niner	607.2-607.8	3.25	Whole core in fair condition - one piece with rough edges 7 inches in length. Core shipped in zip-lock bag.
3/7	Pallet 2 BWBDL	Dewey Lake	208.1-208.7	3.25	Whole core in fair condition - core broken in two pieces, 1.5 and 5.75 inches in length. Core shipped in zip lock bag.
3/7	Pallet 2 DL	Dewey Lake	123.2-123.8	3.25	Whole core in good condition - one piece 7 inches in length. Core shipped in zip-lock bag.
3/7	Pallet 2 DLS-BWBZ	Dewey Lake	202.0-202.55	3.25	Whole core in good condition - one piece 7 inches in length. Core shipped in zip-lock bag.
4/7	Pallet 2 M-4 Top	Forty-Niner	596.5-597.0	3.25	Whole core in fair condition - one piece with rough edges/sides 6.25 inches in length. Core shipped in zip-lock bag.
4/7	Pallet 2 AWBZ-DL	Dewey Lake	176.9-177.55	3.25	Whole core in poor condition - core broken in three pieces, 2.75, 2, and 0.75 inches in length. Core shipped in zip-lock bag.

Table 2: Initial Core Conditions - continued

Box ID	Shipping ID	Formation/ Unit	Depth (ft)	Whole Core Diameter (in)	Conditions/Comments
4/7	Pallet 2 D.L.	Dewey Lake	343.4-344.15	3.25	Whole core in fair condition - core broken in two pieces, 1.75 and 6 inches in length. Core shipped in zip-lock bag.
4/7	Pallet 2 AWBZ-DL	Dewey Lake	172.2-172.7	3.25	Whole core in good condition - core length 5.5 inches. Core shipped in zip-lock bag.
5/7	Pallet 2 A-2	Tamarisk	728.8-729.65	3.25	Whole core in good condition - core length 9.5 inches. Core shipped in zip-lock bag.
5/7	Pallet 2 A-4	Forty-Niner	615.0-615.6	3.25	Whole core in good condition - core length 7.5 inches. Core shipped in zip-lock bag.
5/7	Pallet 2 A-5 top	Forty-Niner	567.1-567.7	3.25	Whole core in good condition - core length 7 inches. Core shipped in zip-lock bag.
5/7	Pallet 2 A-2	Tamarisk	731.3-732.0	3.25	Whole core in fair condition - core length 8 inches and exhibits fractures - gyp-rz - core shipped in zip-lock bag.
6/7	Pallet 2 AWBZ-DL	Dewey Lake	191.7-192.2	3.25	Whole core in fair condition - core length 5.5 inches exhibiting rough edges and friable. Core shipped in zip-lock bag.
6/7	Pallet 2 Magenta	Magenta	641.05 641.75	3.25	Whole core in fair condition - core length 6.75 inches exhibiting rough edges. Core shipped in zip-lock bag.
6/7	Pallet 2 MCTZ	Magenta	622.65 623.1	3.25	Whole core in good condition - core length 5.25 inches. Core shipped in zip-lock bag.
6/7	Pallet 2 A-5	Forty-Niner	581.3-581.9	3.25	Whole core in good condition - core length 7.5 inches. Core shipped in zip-lock bag.
6/7	Pallet 2 Magenta	Magenta	637.9 638.5	3.25	Whole core in poor condition - core length approximately 4 inches with sides falling apart - friable - core shipped in zip-lock bag.
7/7	Pallet 2 A-4	Forty-Niner	621.7-622.3	3.25	Whole core in fair condition - core length 5.5 inches exhibiting rough edges. Core shipped in zip-lock bag.

Table 2: Initial Core Conditions - continued

Box ID	Shipping ID	Formation/ Unit	Depth (ft)	Whole Core Diameter (in)	Conditions/Comments
7/7	Pallet 2 Magenta	Magenta	644.3-644.85	3.25	Whole core in fair condition - core in two pieces with lengths of 4 and 1.75 inches. Core shipped in zip-lock bag.
7/7	Pallet 2 M-4 Middle	Forty-Niner	604.1-604.65	3.25	Whole core in fair condition - core length 6.75 inches exhibiting rough edges. Core shipped in zip-lock bag.
7/7	Pallet 2 A-2 CPT	Tamarisk	681.4-682.0	3.25	Whole core in good condition - core length 7 inches. Core shipped in zip-lock bag.

3 SAMPLE PREPARATION

3.1 Coring and Surface-Grinding

Following inspection of the whole core, it was determined that test specimens had to be undercored since the majority of the whole core exhibited irregular diameters which could have influenced test results. For consistency, even whole core in "good" condition was undercored. Over 95% of the test specimens prepared for this program had nominal diameters of 1.5 inches. A few samples had to be prepared with one-inch diameters, due to fractures and/or material availability. Test specimens were prepared oriented along the axis of the core (i.e., vertical samples) and normal to the core axis (i.e., horizontal samples). All subcoring activities were performed using Odorless Mineral Spirits (OMS) as the circulating/cooling fluid. OMS prevents a sample from drying during preparation and rapidly evaporates from the sample surface following preparation. In addition, the relatively inert characteristics of OMS make it an ideal cutting fluid when moisture-sensitive minerals such as clay, gypsum, and halite are present. The ends of each cylindrical test specimen was machine-ground flat and parallel to a tolerance of ±0.001 inches per inch length.

One vertical and one horizontal test specimen were prepared from each core interval received from the Dewey Lake, Magenta, Forty-Niner, Tamarisk, and the Unnamed Lower Member, with one exception. One anhydrite interval (779.0 - 779.5 ft.) from the Unnamed Lower Member contained many fracture sets which parted during preparation. Hence, no useable test specimen was prepared from this interval. Nearly twenty feet of continuous core were available for preparation from the Culebra. In this case, vertical and horizontal specimens were typically prepared at spacings between six and twelve inches. A listing of the prepared test specimens is

included in Tables 3 through 8. These tables include the specimen identifiers, depths, and rock types. QAPP preparation Worksheet No. 2, for all test samples, is provided in Appendix A. Worksheet No. 2 includes the test specimen's dimensions and parallelism (both ends and sides).

The vertical test specimens were used for porosity determination, gas permeability measurements, electrical properties determinations, and pore volume compressibility measurements. The horizontal specimens were only used for gas and liquid permeability measurements (Table 1 summarizes the tasks performed on a given formation).

3.2 Sample Drying

Following preparation, test specimens were dried in a convection oven set at 60°C. Criteria for weight stabilization were more stringent then ISRM recommendations[1], which define stability as successive mass determinations (4 hr. intervals) differing by less than 0.1% of the sample mass. For this program, all of the samples were dried to between 0 and 0.05% mass change over a 24 hour period. Drying temperature was maintained between 59 and 61°C, with the laboratory humidity ranging from 28 to 55%, for the more than 2880 hours required to dry all of the samples. The majority of the samples reached constant mass within 500 hours, with the laboratory humidity fluctuating between 42 and 49%. Samples containing clay, gypsum and anhydrite took longer to stabilize. Total drying times and mass reduction records during drying, are provided in Appendix A (QAPP Sample Drying Worksheet No. 8).

Three additional Culebra samples were prepared and dried from a core sample provided by SNL later in the program. These samples are also included in Appendix A and Table 3.

[1] *Rock Characterization, Testing and Monitoring: ISRM Suggested Methods*, E.T. Brown (Ed.), 211 p., Pergamon Press, New York. Oven requirements and definitions of dry are given on p. 82.

Table 3: Culebra Test Samples

Depth/Orientation (ft/V,H)	TerraTek ID	Rock Type	Depth/Orientation (ft/V,H)	TerraTek ID	Rock Type
741.35-.6' V	C-1-V	Argillaceous Dolomite	748.3-.55' V	C-12-V	Argillaceous Dolomite
741.2' H	C-1-H		748.45' H	C-12-H	
741.8-.9' V	C-2-V		749.1-.3' V	C-13-V	
741.7' H	C-2-H		749.45' H	C-13-H	
742.0-.2' V	C-3-V		750.0-.2' V	C-14-V	
742.35' H	C-3-H		750.3' H	C-14-H	
743.0-.2' V	C-4-V		756.25-.4' V	C-15-V	
743.25' H	C-4-H		756.1' H	C-15-H	
743.3-.5' V	C-5-V		756.7-.8' V	C-16-V	
743.65' H	C-5-H		756.5-.6' V	C-17-V	
744.25-.5' V	C-6-V		756.9' H	C-17-H	
744.6' H	C-6-H		757.0-.2' V	C-18-V	
745.15-.4' V	C-7-V		759.7' H	C-18-H	
745.0' H	C-7-H		759.1-.35' V	C-19-V	
746.0-.15' V	C-8-V		759.0' H	C-19-H	
745.9' H	C-8-H		759.8-760.0' V	C-20-V	
746.75-747.0' V	C-9-V		760.1' H	C-20-H	
747.25' H	C-9-H		760.2-.4' V	C-21-V	
747.35-.6' V	C-10-V		760.45' H	C-21-H	
747.7' H	C-10-H		750' V*	C-1A-V	
747.75-748.0' V	C-11-V		750' V*	C-2A-V	
748.1' H	C-11-H		750' V*	C-3A-V	

V designation indicates a vertical test sample (sample drilled parallel to the whole core axis).
H designation indicates a horizontal test sample (sample drilled normal to the whole core axis).
* Samples prepared from new core provided by SNL midway through project - depth provided by Y. Behl personal communication - core identified as AIS VPX26-11B.

Table 4: Magenta Test Samples

Depth/Orientation (ft/V,H)	TerraTek ID	Rock Type	Depth/Orientation (ft/V,H)	TerraTek ID	Rock Type
622.85-623.1' V	M-1-V	Microporous Argillaceous Dolomite	641.25-.5' V	M-3-V	Microporous Argillaceous Dolomite
622.65-623.1' V*	M-1A-V		641.15' H	M-3-H	
622.75' H	M-1-H		644.5-.75' V	M-4-V	
638.15-.4' V	M-2-V		644.4' H	M-4-H	
638.0' H	M-2-H		na	na	

V designation indicates a vertical test sample (sample drilled parallel to the whole core axis).
H designation indicates a horizontal test sample (sample drilled normal to the whole core axis).
* Second vertical sample prepared from this depth interval due to jacket failure during permeability test on sample M-1-V.

Table 5: Dewey Lake Test Samples

Depth/Orientation (ft/V,H)	TerraTek ID	Rock Type	Depth/Orientation (ft/V,H)	TerraTek ID	Rock Type
123.35-.6' V	DL-1-V	Siltstone/ Sandstone	202.15-.4' V	DL-5-V	Siltstone/ Sandstone
123.3' H	DL-1-H		202.1' H	DL-5-H	
172.3-.55' V	DL-2-V		208.35-.6' V	DL-6-V	
172.6' H	DL-2-H		208.2' H	DL-6-H	
177.3-.45' V	DL-3-V		343.7-.95' V	DL-7-V	
177.05' H	DL-3-H		344.05' H	DL-7-H	
191.95-192.2' V	DL-4-V		562.6-.85' V	DL-8-V	
191.85' H	DL-4-H		562.5' H	DL-8-H	

V designation indicates a vertical test sample (sample drilled parallel to the whole core axis).
H designation indicates a horizontal test sample (sample drilled normal to the whole core axis).

Table 6: Forty-Niner Test Samples

Depth/Orientation (ft/V,H)	TerraTek ID	Rock Type	Depth/Orientation (ft/V,H)	TerraTek ID	Rock Type
567.35-.6' V	FN-1-V	Anhydrite	607.3' H	FN-4-H	Claystone
567.25' H	FN-1-H	Anhydrite	615.15-.4' V	FN-5-V	Anhydrite
581.5-.75' V	FN-2-V	Anhydrite	615.05' H	FN-5-H	Anhydrite
581.4' H	FN-2-H	Anhydrite	621.9-622.15' V	FN-6-V	Anhydrite
596.65-.9' V	FN-3-V	Claystone	621.8' H	FN-6-H	Anhydrite
596.55' H	FN-3-H	Claystone	604.2-.45' V	FN-7-V	Claystone
607.35-.6' V	FN-4-V	Claystone	604.55' H	FN-7-H	Claystone

V designation indicates a vertical test sample (sample drilled parallel to the whole core axis).
H designation indicates a horizontal test sample (sample drilled normal to the whole core axis).

Table 7: Tamarisk Test Samples

Depth/Orientation (ft/V,H)	TerraTek ID	Rock Type	Depth/Orientation (ft/V,H)	TerraTek ID	Rock Type
664.85-665.1' V	T-1-V	Anhydrite	721.0' H	T-4-H	Claystone
664.8' H	T-1-H	Anhydrite	724.15-.4' V	T-5-V	Anhydrite
681.6-85' V	T-2-V	Anhydrite	724.05' H	T-5-H	Anhydrite
681.5' H	T-2-H	Anhydrite	729.0-.25' V	T-6-V	Anhydrite
713.05-3' V	T-3-V	Claystone	728.9' H	T-6-H	Anhydrite
712.8' H	T-3-H	Claystone	731.75-732.0' V	T-7-V	Anhydrite
721.2-.35' V	T-4-V	Claystone	731.4' H	T-7-H	Anhydrite

V designation indicates a vertical test sample (sample drilled parallel to the whole core axis).
H designation indicates a horizontal test sample (sample drilled normal to the whole core axis).

Table 8: Un-Named Lower Member Test Samples

Depth/Orientation (ft/V,H)	TerraTek ID	Rock Type
762.55-.8' V	UNM-1-V	Blue-Gray Claystone
762.45' H	UNM-1-H	Blue-Gray Claystone
770.3-.55' V	UNM-2-V	Red Claystone
770.2' H	UNM-2-H	Red Claystone
773.1-.35' V	UNM-3-V	Anhydrite
773.0' H	UNM-3-H	Anhydrite

V designation indicates a vertical test sample (sample drilled parallel to the whole core axis).
H designation indicates a horizontal test sample (sample drilled normal to the whole core axis).
Unable to obtain samples from depth 779.0-779.5' (un-named member anhydrite core) due to fractures.

4 TEST PROCEDURES

4.1 Porosity

Background

Porosity was determined from measurements of grain volume and bulk volume. Helium expansion was used to determine the grain volume, using the Boyles' Law technique. Bulk volume was determined by measuring the specimen's dimensions with calipers. The bulk volume, grain volume and mass information were used to compute porosity and grain density. Bulk density and grain density can also be used to calculate porosity as long as a material is reasonably homogeneous and the measurements are performed on subsamples of the same core.

The samples were tested following drying to constant mass. Gas porosimetry (for grain volume) is based on Boyle's Law, which holds that for an ideal gas, at constant temperature, the volume of the gas will vary inversely with pressure:

$$\frac{P_1}{P_2} = \frac{V_2}{V_1} \qquad (1)$$

where P_1 is the initial pressure in the initial volume V_1 and P_2 is the final pressure in the final volume V_2. The porosimeter consists of a steel vessel connected to a gas reservoir through high pressure tubing.

Calibration of the custom-fabricated gas expansion porosimeter is performed daily using a series of steel billets of known volume. The calibration consists of sequentially increasing the volume, V_2, by known amounts. Hence, as V_2 increases the ratio P_1/P_2 also increases. Linear regression is performed to determine the relationship between the measured ratio, P_1/P_2, and the sample volume such that:

$$V_g = m\frac{P_1}{P_2} + b \qquad (2)$$

V_g is either the effective or total grain volume, depending on the sample type (crushed or intact). The experimentally determined slope *m* thus gives the proportionality between grain volume and pressure ratio; whereas, the V_g intercept (*b*) represents the zero offset (i.e., due to the "dead volume" in the porosimeter). These values of *m* and *b* are used in subsequent measurements of grain volume (see Worksheet No. 6).

The bulk volumes of the porosimeter billets (used to vary V_2) are calibrated using Archimedes' principle (see Worksheet No. 4, Appendix B).

Density Determinations

Dry bulk density was measured according to ISRM procedures[2]. The sample's mass is determined and then the bulk volume is measured. Specimen bulk volume was determined by direct measurement on the cylindrical specimens using calipers. Grain density was determined from direct grain volume measurements using gas pycnometry (as described above). Note that if a test sample is pulverized prior to the measurement, calculation of the total porosity can be performed (i.e., the sum of the interconnected and occluded pores). If the measurement is performed on an intact core specimen, only the interconnected porosity will be determined. The former is known as the total matrix porosity, and the latter is known as the effective porosity. Similarly, the grain densities determined from pulverized samples and intact samples are known as the true grain density and effective grain density, respectively. For this program only effective properties were determined.

[2] *Rock Characterization, Testing and Monitoring: ISRM Suggested Methods*, E.T. Brown (Ed.), 211p., Pergamon Press, New York. Procedures for the fluid displacement method for determination of bulk volume of solid and porous samples are outlined on p. 82.

Test Procedures

Grain volume, V_g, was determined using a Boyle's Law double cell technique[3]:

- Calibrate porosimeter using appropriate sized steel billets with known volumes. A correlation coefficient (R value) greater than or equal to 0.99998 is acceptable;
- Measure the sample's weight;
- Briefly open the reference cell valve to allow pressure to equilibrate;
- Insert the sample into the porosimeter (either an intact cylindrical sample or a metal holder with pulverized sample) and record the initial pressure, P_1 (nominally 100 psi), with the reference valve and the sample chamber valve closed;
- Open the sample chamber valve;
- Record the equilibrated pressure, P_2, (equilibration time varies between samples but typically ranges from 10 to 30 minutes).
- Complete Worksheet No. 6.

Bulk volume, V_{bulk}, was determined using the caliper method:

- Measure and record the cylindrical sample weight;
- Measure and record the diameter at six different locations;
- Measure and record the length at four different positions;
- Calculate the bulk volume and bulk density using Worksheet No. 3.

Analysis Procedures

Effective porosity was calculated from the foregoing measurements using:

[3]*Rock Characterization, Testing and Monitoring: ISRM Suggested Methods*, E.T. Brown (Ed.), 211p., Pergamon Press, New York. Procedure for determination of grain volume using Boyle's law double cell technique is outlined on p. 83.

$$\phi = 1 - \frac{\rho_d}{\rho_g} \tag{3}$$

where ϕ is the porosity (fractional), ρ_d is the dry bulk density, and ρ_g is the grain density. The QAPP provides more detailed information pertaining to the equipment used to measure porosity. Caliper measurements, porosimeter billet calibrations and grain volume measurement worksheets are included in Appendix B (QAPP Worksheets No. 3, 4 and 6).

4.2 Single-Phase Gas Permeability Tests (Absolute Permeability to Gas)

A modified Hassler-type hydrostatic core holder was used for all permeability measurements for this program. The core holder is a cylindrical steel pressure vessel rated to 15,000 psi, which can accommodate samples with diameters up to 4 inches and lengths up to 6 inches. The cylindrical test specimen was inserted into a Viton rubber sleeve of appropriate diameter and length, which isolated the specimen from the confining fluid (Paratherm oil) and provided a seal along the cylinder sides. Typically, a high pressure pump is utilized to supply the confining pressure. After the designated confining pressure level is reached, the pressure is shut in by closing a valve. For this program, which required long-term stability of pressures, a combination high pressure pump and a gas pressure backed piston accumulator was used to control the confining pressure; minimizing pressure variation due to room temperature fluctuation.

All permeability measurements were done in the axial direction (i.e., along the core axis). Horizontal permeability was determined for samples prepared with the axial direction parallel to the horizontal direction (samples prepared normal to the core axis). To ensure pore fluid dispersion across the sample faces, two 60 × 60 mesh stainless steel screens were placed on each sample end. Stainless steel endcaps, with supply ports and dispersion grooves were inserted into the sleeve and secured with safety lock wire or hose clamps. High pressure stainless steel tubing passing through the pressure vessel end closure allowed pore fluid to flow through the endcaps. Absolute permeability to gas was measured at a net effective stress based on 1 psi/ft depth (overburden stress gradient), and a pore pressure of approximately 50 psi. Tests were conducted at ambient temperature (23°C) using nitrogen gas as the flowing fluid.

4.2.1 Test Procedures

Procedures used for measurement of gas permeability were based upon ASTM recommendations[4] and were as follows:

[4] *Standard Test Method for Permeability of Rocks by Flowing Air*, D 4525-90, American Society for Testing Materials, 1990.

- Measure the sample's diameter and length using calipers;

- Jacket the sample in a pliable elastomer sleeve;

- Mount stainless steel end caps with supply ports, dispersion grooves, and 60 × 60 mesh stainless steel screens on the sample ends;

- Attach stainless steel high pressure tubing to both endcaps to supply and vent the pore fluid (nitrogen gas);

- Install the sample stack vertically in an hydrostatic core holder;

- Apply the appropriate confining pressure (between 250 and 1000 psi) using Paratherm oil as the confining fluid. Allow the temperature to stabilize;

- Apply regulated gas pressure at the upstream end. Impose a gas pressure greater than 50 psig at the upstream end sufficient to cause measurable fluid flow along the sample length. If necessary, adjust the confining pressure to maintain the specified net effective stress;

- Monitor pressures to establish attainment of steady-state conditions, defined by differential pressure changes of no more than ±2.5% in 30 minutes;

- Measure the exit flow rate (at barometric pressure) by using a stop watch (to 0.01 second) to time a travelling meniscus of soap film in an appropriately ranged, horizontally mounted pipette. Take a minimum of three flow rate measurements.

- Complete Worksheet No. 9.

4.2.2 Analysis Procedures

Gas permeability, k_g, was calculated from the following equation:

$$k_g = -\frac{Q_b}{A}\left(\frac{2P_bL}{P_2^2-P_1^2}\right)\mu = \frac{Q_b}{A}\frac{P_b}{P_m}\frac{L}{\Delta P}\mu \qquad (4)$$

where:

Q_b = the volumetric flow rate measured at barometric pressure;
P_b = barometric pressure;
A = the cross-sectional area of the sample;
P_1, P_2 = the gas pressures at the upstream and downstream ends (respectively);
μ = the gas viscosity;
L = the length of the sample; and,
P_m = $1/2(P_1+P_2)$.

The term P_b/P_m adjusts Q_b to the volumetric flow at the mean pore pressure. Appendix C provides the gas permeability QAPP worksheet No. 9 for all samples tested.

4.3 Single-Phase Liquid Permeability Tests (Absolute Liquid Permeability)

Absolute liquid permeabilities were measured using the test conditions/procedures discussed for gas permeability. OMS was used as the flowing fluid. The vessel, endcaps, jackets, and pressure transducers, which were used during the measurement of liquid single-phase permeability, are described in the previous section (Gas Permeability). The injection pressure for the fluid (OMS) was provided by an ISCO 500D syringe pump. Exit flow rates were measured in appropriately ranged pipettes. Figure 1 is a schematic of the flow system used for both liquid and gas permeability measurements.

Only a few horizontal samples were designated for liquid permeability measurements. These were predominantly clay-rich samples whose vertical counterparts were mechanically loaded during pore volume compressibility testing. It was mutually agree between TerraTek and the SDR that only gas permeability measurements would be performed on the vertical samples prior to mechanical testing. Permeability testing after compressibility measurements could have been misleading.

4.3.1 Test Procedures

The procedures used for liquid permeability measurements[5] were:

- Measure the sample diameter and length using calipers;
- Jacket the sample in a pliable elastomer sleeve;

[5]General guidelines for measurement of liquid permeability may be found in, for example, *Test Methods for Evaluating Solid Waste: Volume IC: Laboratory Manual Physical/Chemical Methods: Method 9100 Saturated Hydraulic Conductivity, Saturated Leachate Conductivity, and Intrinsic Permeability,* 3rd ed., U.S. Environmental Protection Agency, Office of Solid Waste and Emergency Response, Washington DC, 1986.

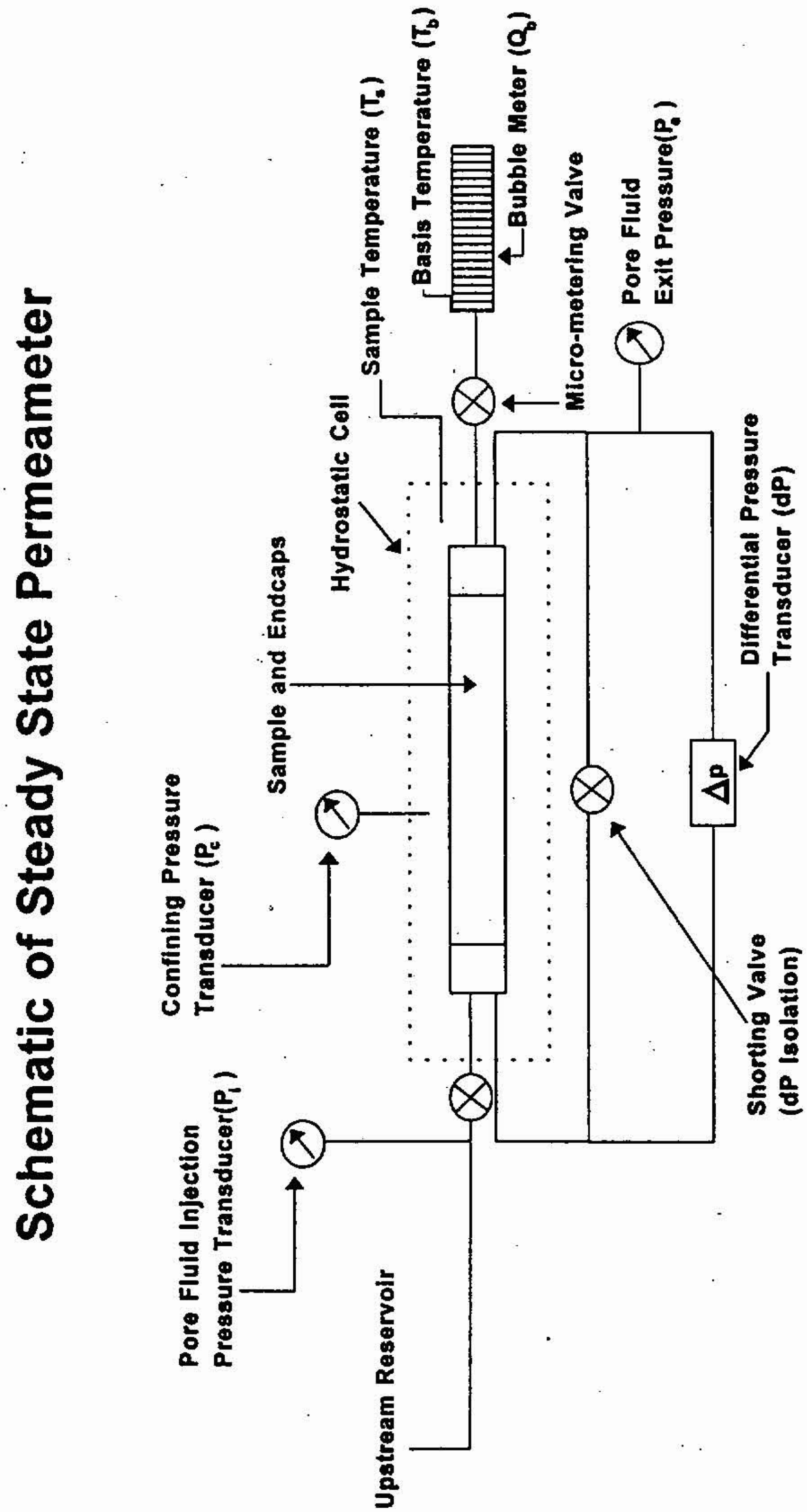

Figure 1: Schematic of system for measuring gas and liquid permeabilities.

- Mount stainless steel endcaps with supply ports, dispersion grooves, and 60 × 60 mesh stainless steel screens on the sample ends;

- Attach stainless steel high pressure tubing to both endcaps to supply pore fluid (OMS);

- Install sample stack vertically in hydrostatic core holder;

- Apply the appropriate confining pressure (1 psi/ft depth) using Paratherm oil as the confining fluid;

- Increase pore fluid pressure to approximately 50 psi and allow system to stabilize;

- Following equilibration, pore fluid flow is initiated by opening the upstream inlet valve and the downstream exit valve. The exit flow rate is controlled by a micro-metering valve;

- Once steady-state flow is achieved, the mean pore pressure is computed and then adjustments to the confining pressure are made in order to provide the target net effective hydrostatic stress (1.0 psi/ft);

- Monitor pressures to establish attainment of steady-state, defined by differential pressure changes of no more than ±2.5% in 30 minutes (note this criterion may be modified as necessary depending upon permeability);

- Measure exit flow rate (at barometric pressure) by using a stop watch (to 0.01 second) to time a travelling meniscus in an appropriately ranged, horizontally mounted pipette. Take a minimum of three flow rate measurements.

- Remove the sample from the vessel.

- Complete Worksheet No. 10.

More detailed procedural descriptions for both gas and liquid permeabilities are provided in the test technician's scientific notebooks.

4.3.2 Analysis Procedures

Using the steady-state technique, absolute permeability to OMS, k_l, was calculated as:

$$k_1 = \left(\frac{Q\mu}{A}\right)\left(\frac{L}{\Delta P}\right) \quad (5)$$

where:

Q	= the volumetric flow rate;
A	= the cross-sectional area of the sample;
L	= the length of the sample in the macroscopic flow direction;
ΔP	= P_1-P_2, which is the hydrostatic pressure drop across the sample length; and
μ	= the viscosity of the fluid.

Pressure drops across the core were chosen so that laminar flow was assured. QAPP liquid permeability worksheet No. 10 is provided in Appendix C.

4.4 Formation Factor - Electrical Resistivity

Formation Factor (F_R) was determined for all vertically oriented Culebra samples using formation fluid supplied by SNL at the confining pressures used for the permeability measurements.

4.4.1 Equipment and Testing Procedures

Reservoir water saturation is generally estimated from Archie's equations, 1942[6], 1947[7].

$$F_R = a\phi^{-m} = \frac{R_o}{R_w} \quad (6)$$

where:

F_R - Formation Factor;
a - generally assumed to be 1.0;

[6] Archie, G.E., "The Electrical Resistivity Log as an Aid in Determining Some Reservoir Characteristics," Trans AIME, Vol., 146, 1942.

[7] Archie, G.E., "Electrical Resistivity - An Aid in Core Analysis Interpretation," Bull. AAPG, No. 2, 1947.

ϕ - Porosity;
m - Cementation Factor;
R_o - Sample resistivity, containing water (brine) only; and,
R_w - Formation water (brine) resistivity.

The foregoing equations were originally developed for strongly water-wet, clean formations (sandstone or unconsolidated sand with no clay present). Under those conditions, a value of 2 for m and for n generally gives acceptable results for calculating the water saturation, S_w. Correlations accommodating shaliness were proposed by Hill and Milburn, 1956[8], Waxman and Smits, 1966[9], and Waxman and Thomas, 1974[10].

As ideal scenarios are rarely encountered, the coefficients m and n are mainly determined from laboratory testing performed on samples assumed to be representative of the medium to be investigated. It is important that the testing is performed at conditions specifically representing the formation environment (fluid composition, effective stress, temperature...)[11]. TerraTek's resistivity system is an evolutionary modification of equipment described by Waxman and Thomas, 1974[10], and Longeron et al., 1986[12].

TerraTek's resistivity cells are configured to provide core resistivity measurements using the four electrode method. However, when available samples are shorter than two inches in length (one inch diameter sample), two electrode measurements are performed. Two and four electrode measurements may give equally good results when performed correctly. With two electrode methods, the current and potential electrodes are combined. However, two electrode systems may give rise to errors due to poor rock-electrode contacts. Four electrode systems have separate current and potential electrodes to avoid contact resistance. In the four electrode configuration sample homogeneity and uniform fluid distribution are critically important due to the reduced volume of core measured. Resistivity equipment is calibrated prior to testing using precision

---

[8] Hill, J.J. and J.D. Milburn, "Effect of Clay and Water Salinity on Electro-chemical Behavior of Reservoir Rocks," Trans AIME, V. 207, 1956.

[9] Waxman, M.H. and L.J. Smits, "Electrical Conductivities in Oil-Bearing Shaly Sands," SPEJ, June 1966.

[10] Waxman, M.H. and E.C. Thomas, "Electrical Conductivities in Shaley Sands. I. The Relationship Between Hydrocarbon Saturation and Resistivity Index. II. The Temperature Coefficient of Electrical Conductivity," JPT, February 1974.

[11] Longeron, D.G., "Laboratory Measurements of Capillary and Electrical Properties of Rock Samples at Reservoir Conditions: Effect of Some Parameters," 1990 SCA Conference Paper No. 9023.

[12] Longeron, D.G., Argaud, M.J. and J.P. Feraud, "Effect of Overburden Pressure, Nature and Microscopic Distribution of the Fluids on Electrical Properties of Rock Samples," 61st SPE Annual Technical Conference and Exhibition, New Orleans, October 1986.

resistors. The majority of the formation factors for SNL were determined using the four electrode method.

Sample Preparation/Dimensions

- Vertically oriented Culebra samples were tested. These samples were initially used for porosity and gas permeability measurements.
- Where possible, the samples were prepared with relatively uniform lithology. Comments are made describing the nature of the sample's heterogeneity.
- The typical SNL test sample size was 1.5 inches in diameter by between 2 and 3 inches in length.
- It is preferred that the adopted length-to-diameter ratio (for a two electrode system) allows a minimum electrode spacing of 1.5 times the sample diameter.
- For obviously heterogeneous specimens, the electrode spacing will exceed 1.5 times the sample diameter.
- The length and diameters of the samples must be measured to within a tolerance of 0.001 inches. The diameter and length are determined by geometric averaging of six individual measurements.

Sample Mounting/Saturation

Each sample was jacketed in a Viton membrane, with three voltage electrodes for (two or four-pole) resistivity measurements. One of the electrodes is at the sample's longitudinal midpoint; the two others are 0.75 inch on either side of this one. The jackets were slightly oversized (1.530 inches) in order to accommodate nominally 1.500 inch diameter samples.

Formation brine supplied by SNL was used. De-aerated brine was siphoned into the evacuated saturation system. On competent samples, saturation is confirmed gravimetrically (as was the case for the SNL samples). Worksheet No. 11 (Appendix D) is the sample saturation data sheet including the criteria for a saturated sample.

With the saturated sample placed inside the Viton jacket, a diffusion endcap was placed in contact with one end and a porous plate endcap was installed against the other end. The Viton jacket was sealed to the endcaps with hose clamps. The endcaps were connected to insulated pore pressure lines that run through the closure for the pressure cell. Each sample was placed in the hydrostatic pressure cell and a minimum confining pressure (usually 200 psi) was applied to ensure intimate contact and sealing.

The samples were allowed to ionically equilibrate with the supplied brine. Equilibrium was assessed by monitoring stabilization in F_R with time. Calculation of the formation factor is shown in Equation (6). Data and calibration information are entered in QAPP Worksheets 12 and 13, (Appendix D).

4.5 Pore Volume Compressibility

Pore volume compressibility was determined from uniaxial strain compaction testing. Vertical test specimens from the Forty-Niner, Tamarisk, Magenta and the Unnamed Lower Member were selected for pore volume compressibility testing.

4.5.1 Pore Volume Compressibility Apparatus and Related Equipment

Compressibility testing was performed in one of TerraTek's triaxial vessels (refer to Figure 2). A typical machine is stiff, with servo-controlled actuators and intensifiers. Each sample was placed between ported stainless steel endcaps and jacketed with a Teflon sleeve. The sleeve was used to separate the pore fluid from the confining fluid so that these boundary conditions can be controlled independently. For these tests, the pore fluid pressure was vented to atmosphere. The stainless steel endcaps have central holes and face grooves to allow fluid to flow in and out of the sample. Each instrumented sample is placed into a pressure vessel for compressibility measurements under hydrostatic-uniaxial strain loading. Hydrostatic loading was initially used to a target stress between 400 and 650 psi (based on a vertical stress gradient of 1 psi/ft depth minus 150 psi pore pressure). These values were chosen so that measurable strain occurred during hydrostatic loading. The premise for the hydrostatic loading is that, since these samples are from a relatively shallow depth (less than 1000 vertical feet), the horizontal stresses may be as high as the vertical stress. Hence, hydrostatic loading may provide a more realistic compressibility response. Under uniaxial strain boundary conditions, the axial stress was increased while maintaining constant radial strain (zero radial deformation) by applying a confining pressure. The test was terminated when the axial stress reached a maximum vertical stress of 1500 psi.

Axial and radial strains were monitored using Linear Variable Displacement Transducers (LVDT) and strain-gaged cantilever systems, providing the accuracy required for the precise strain measurement needed for this type of testing. Accuracies for confining pressure, pore pressure, axial stress, and strain were ±0.5%, ±.25%, ±.25%, and ±0.001%, respectively.

4.5.2 Calibration Procedures

Initial calibration of the LVDT's (used to measure axial strain) and the cantilever sets (used to measure radial strain) was performed by displacing the cantilevers to at least the maximum

expected displacement, using either a precision height gauge or an inside micrometer. Additional calibration is required to account for the effect of confining pressure on the gages and the cantilevers themselves. The effect of the jacket and endcap compressibility must also be considered. These "pressure effects" can be determined from a single calibration. Finally, the effect of load on the endcap is considered. A designated calibration sequence is performed by placing a gauged and cantilever-instrumented 6061 aluminum billet inside the pressure vessel and hydrostatically loading/unloading this sample arrangement three times. The known properties of the gaged billet are compared to those measured by the cantilever systems. The resultant calibration factor is then used for subsequent testing. Additional calibration procedures are documented in the QAPP for contract AA-2896.

4.5.3 Test Procedures

Procedures for measuring pore volume compressibility, using hydrostatic/uniaxial strain loading path were as follows:

- Measure the sample's diameter (average of six measurements) and length (average of four measurements) using calipers;
- Place the sample between the steel endcaps with a supply port on the bottom endcap;
- Jacket the sample and endcaps with heat-shrinkable Teflon sleeves;
- Attach stainless steel high pressure tubing to the bottom endcap to vent any pore pressure to the atmosphere;
- Install the axial LVDT's and radial cantilevers and place the sample stack into the triaxial vessel;
- Apply a hydrostatic confining pressure. This was based on the sample depth (1 psi/ft gradient minus an estimated nominal pore pressure of 150 psi). For example, a sample from a depth of 650 ft. would be subjected to a confining pressure of 500 psi. The confining pressure was applied at a rate of 0.25 psi/s, until the target confining pressure was obtained;
- Increase the axial stress difference at a rate of 0.25 psi/s under uniaxial strain boundary conditions (zero lateral deformation). Continue axial loading until σ_1 is approximately 1500 psi;
- Once the σ_1 target of 1500 psi is reached, remove the axial stress difference under uniaxial strain conditions at a rate of -0.25 psi/s until the axial stress difference is zero;

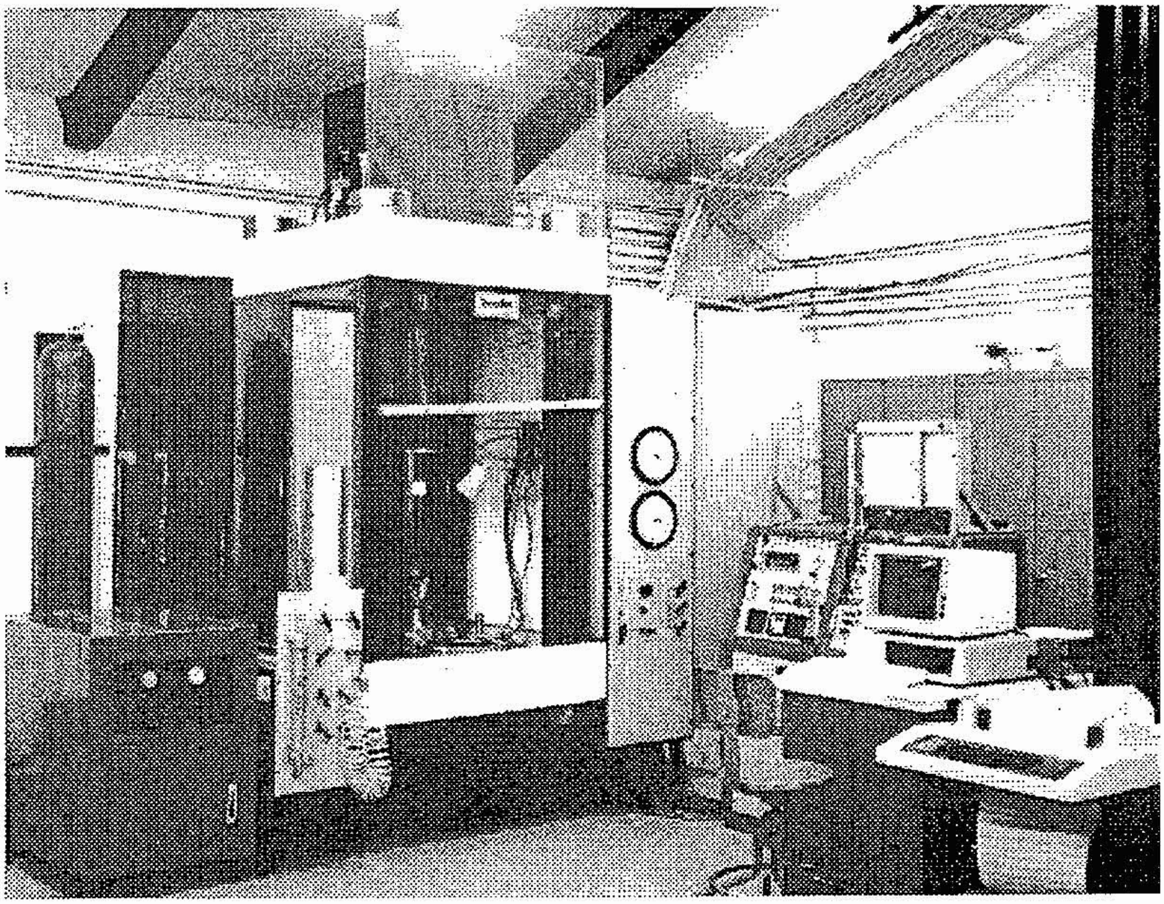

Figure 2: Typical triaxial testing frame.

- Hydrostatically unload the test sample at a stress rate of -0.25 psi/s to zero. The test was completed at this point.

4.5.4 Analysis Procedures

The pore volume compressibility over various mean effective stress ranges was calculated as follows:

$$C_b = \frac{\partial \varepsilon_v}{\partial \sigma'_m} \qquad (7)$$

where:

C_b = is the bulk compressibility, psi^{-1},

ε_v = is the volumetric strain, and
σ'_m = is the mean effective stress, psi.

The volumetric strain is:

$$\varepsilon_v = \varepsilon_{r_1} + \varepsilon_{r_2} + \varepsilon_a \tag{8}$$

where:

ε_{r1} = is a radial strain (measured) in one direction,
ε_{r2} = is a radial strain (measured) in a direction orthogonal to ε_{r1}, and,
ε_a = is the axial strain.

The mean effective stress is:

$$\sigma'_m = \frac{\sigma'_1 + 2\sigma'_3}{3} \tag{9}$$

where:

$\sigma_i' = \sigma_i - \alpha P_p$

in these tests the pore pressure (P_p) is maintained at zero psi, so that:

σ_i' = σ_i
σ_i = total stress, (psi),
σ_i' = effective stress, (psi),
σ_1' = effective axial stress, (psi), and
σ_3' = effective confining pressure, (psi).

Presuming that $C_g << C_b$ (the grain compressibility is very much smaller than the bulk compressibility):

$$C_p = \frac{C_b}{\phi} \tag{10}$$

where:

C_p = the pore volume compressibility (psi^{-1}), and,

ϕ = the porosity (fraction).

5 RESULTS

5.1 Porosity and Permeability

Porosity and permeability results are presented in Tables 9 through 16. Two gas permeability values are provided in the data tables. One value represents the hand-calculated value (which was reported in the progress reports); the other value was calculated using a spreadsheet program. The hand-calculated and the spreadsheet calculated data are essentially the same. In a few cases some of the measured permeabilities were determined from flow rates that had exceeded 3 cm^3/s. Past experience has indicated that turbulent flow may result, which correspondingly may significantly affect the differential pressure measurement when flow rates exceed 3 cm^3/s. In this case, the resulting estimated permeability is low. To correct this, a lower ΔP range transducer was needed (and subsequently used) at a lower flow rate. Initial permeability tests with flow rates that had exceeded 3 cm^3/s are identified in the tables by parenthesis with a number. The actual flow rate used is shown in Table 9. In some instances, the flow rate was exceptionally high (e.g., 57 cm^3/s), in which case the error caused by turbulence would be the highest. After installing a low pressure ΔP transducer, gas permeability measurements were repeated for several test samples where flow rates exceeded 3 cm^3/s. After remeasuring the permeability of several samples using the low pressure ΔP, it was observationally determined that gas permeabilities less than 9 md were satisfactory (there was no appreciable change between the low and higher pressure ΔP transducers). Any samples with permeabilities greater than 9 md were measured with the low pressure ΔP. In a few instances an exceptionally high permeability was measured (e.g., several Dewey Lake samples had $K > 100$ md). For these particular samples, the flow rate may still be too high resulting in a potentially low estimate of permeability. All pertinent permeability data including flow rates is provided in the Worksheets in Appendix C.

Magenta sample M-1-V was contaminated with oil due to a jacket failure during the permeability measurement. Attempts were made to remove the oil using Dean-Stark (toluene flush) extraction techniques. Following this cleaning process, the porosity increased substantially from 2.7% to approximately 10%. The combination of oil contamination and Dean-Stark cleaning apparently changed the pore volume of the test specimen. A second sample was taken adjacent to where sample M-1-V had been prepared. Following drying, porosity, permeability and pore volume compressibility testing were conducted on the duplicate M-1-V sample, denoted as M-1A-V.

Initially, it had been intended to measure liquid permeability on all claystone samples; vertical and horizontal. There was concern that flowing liquid and excessive handling could alter the samples before compressibility testing. To expedite testing, measurements of gas permeability for the vertical claystone samples followed by immediate installation in the pressure cell for pore volume compressibility determination was performed. The scenario here was to reduce any risk of damaging the delicate claystone samples from subsequent liquid permeability measurements

and handling. Unfortunately, it was impossible to measure the liquid permeability on the post-test vertical samples due to the irreversible compaction that had occurred. Hence, liquid permeability measurements were only performed on the horizontal claystone samples. The results for the liquid permeabilities, comprising only seven horizontal samples, are presented in Tables 14, 15 and 16.

5.1.1 Composite Accuracy For Permeability Measurements

- Length error ±0.001 inches (nominal 3.000")
- Diameter error ±0.001 inches (nominal 1.500")
- Barometric pressure error ± 1/2% F.S. (17 psia)
- Temperature error ± 1%
- Flow rate error ± 4%
- Differential pressure error ± 1/2%

Permeability	Flow Measurement*1	Differential Pressure*2	Relative Variation
High	500 ml pipette (nominal rate of 250 cm^3/min)	100 psid, 15 psid transducers	0.937 - 1.088
Low	1 ml pipette (nominal rate of 0.5 cm^3/min)	100 psid, 15 psid transducers	0.942 - 1.082

*1 4% error assumed.
*2 0.5% error assumed.

- very rudimentary analyses were undertaken by varying all parameters and calculating permeability for two assumed flow rates. This gives the worst possible combinations if all errors are multiplicatively maximized.

- In the relative variation column, no error gives a value of 1.000.

- This was a generic analysis. If other equipment (for example, a lower range differential pressure transducer) was used, as was the case, the error is reduced.

- NOTE: This analysis is not a rigorous statistical evaluation and should only be used as such.

Table 9: Samples with Initial Flow Rates Exceeding 3 cm^3/s.

Sample ID (number)	Flow Rate - Q_b (cm^3/s)	Sample ID (number)	Flow Rate - Q_b (cm^3/s)
C-8-V (1)	29.5	C-20-H (7)	3.3
C-13-V (2)	6.7	C-21-H (8)	8.9
C-17-V (3)	57.5	C-1A-V (9)*	10.6
C-18-V (4)	15.0	C-3A-V (10)*	20.3
C-19-H (5)	12.3	DL-2-V (11)	4.5
C-20-V (6)	5.9		

*Yugal Behl Culebra test samples.

Table 10: Culebra - Preliminary Data and Final Spreadsheet Determined Results
Yugal Behl's Test Samples

ID	Effective Porosity (%)	Permeability (md)			
		Vertical	Horizontal	Vertical+	Horizontal+
C-1A-V	17.3	10.3(9)/11.6	na	10.3/11.6	na
C-2A-V	13.2	1.36	na	1.36	na
C-3A-V	22.4	19.5(10)/22.9	na	19.5/22.9	na

+Permeability calculated using a spreadsheet program. The second permeability value is the repeated measurement using a lower flow rate. Intuitive cut-off for low flow/low ΔP measurements was 9 md.

Table 11: Culebra - Preliminary Data and Final Spreadsheet Determined Results

ID	Effective Porosity* (%)	Permeability (md)			
		Vertical	Horizontal	Vertical+	Horizontal+
C-1	14.7	0.0918	0.0495	0.0917	0.0495
C-2	13.7	0.0682	0.0214	0.0681	0.0214
C-3	13.4	0.0152	0.0104	0.0152	0.0104
C-4	17.4	0.0731	0.0468	0.0731	0.0468
C-5	13.3	0.0168	0.417	0.0168	0.418
C-6	10.0	0.0390	0.0241	0.0390	0.0241
C-7	10.9	0.996	0.103	0.994	0.103
C-8	10.0	58.2(1)/83.5	0.0139	58.2/83.5	0.0139
C-9	9.8	3.79	0.00204	3.79	0.00203
C-10	8.6	0.00327	0.00287	0.00328	0.00287
C-11	10.2	0.00345	0.0140	0.00346	0.0139
C-12	9.4	0.00499	0.867	0.00498	0.866
C-13	28.1	6.67(2)	0.0206	6.68	0.0206
C-14	9.1	0.00760	0.0864	0.00761	0.0863
C-15	19.5	3.00	0.0334	3.00	0.0333
C-16	15.2	0.0302	na	0.0302	na
C-17	26.6	38.3(3)/69.6	0.00757	38.3/69.6	0.00757
C-18	13.8	15.4(4)/18.3	1.20	15.4/18.3	1.20
C-19	19.7	1.28	14.9(5)/17.2	1.27	14.8/17.2
C-20	19.9	5.64(6)	3.93(7)	5.64	3.93
C-21	15.0	2.42	9.19(8)/9.82	2.41	9.19/9.81

+Permeability calculated using a spreadsheet program. The second permeability value is the repeated measurement using a lower flow rate. Intuitive cut-off for low flow/low ΔP measurements was 9 md.

* Effective Porosity measurements were made on vertical Culebra core plugs.
Lucy Meigs
12/2/96

Table 12: Dewey Lake - Preliminary Data and Final Spreadsheet Determined Results

ID	Effective Porosity (%)	Permeability (md)			
		Vertical	Horizontal	Vertical+	Horizontal+
DL-1	14.9	0.0197	0.0399	0.0197	0.0399
DL-2	21.5	5.84(11)	208*	5.84	208
DL-3	23.2	69.3*	911*	69.2	912
DL-4	24.8	0.515	98.2*	0.515	98.1
DL-5	3.5	0.00239	0.00321	0.00239	0.00321
DL-6	11.6	0.00496	0.272	0.00496	0.272
DL-7	5.4	0.000720	0.0655	0.000720	0.0655
DL-8	9.4	0.0274	0.169	0.0274	0.169

*Measurement performed with low range ΔP transducer (ΔP = 1.6 psi, Q = 9 cm^3/s). However, we suspect that an even lower ΔP transducer should be used for an accurate permeability.

Table 13: Magenta - Preliminary Data and Final Spreadsheet Determined Results

ID	Effective Porosity (%)	Permeability (md)			
		Vertical	Horizontal	Vertical+	Horizontal+
M-1	2.7	0.00489*	0.00119	0.00489	0.00119
M-2	25.2	0.534	1.04	0.534	1.04
M-3	16.6	0.0268	0.0728	0.0268	0.0728
M-4	10.6	0.00383	0.0204	0.00382	0.0204
M-1A	10.1	0.0108	na	0.0108	na

+Permeability calculated using a spreadsheet program.
*Permeability determined following Dean-Stark cleaning. Hence, permeability value is suspect.

Table 14: Forty-Niner - Preliminary Data and Final Spreadsheet Determined Results

ID	Effective Porosity (%)	Permeability (md)				Liquid Permeability (md)
		Vertical	Horizontal	Vertical+	Horizontal+	Horizontal+
FN-1	0	59.4 E-6	48.6 E-6	59.3 E-6	48.6 E-6	-
FN-2	0.15	2.67 E-6	72.3 E-6	2.67 E-6	72.3 E-6	-
FN-3	23.5	0.0288	27.9	0.0287	27.9	4.19
FN-4	9.1	0.0174	0.196	0.0173	0.196	0.0737
FN-5	0.2	0.000113	0.000139	0.000113	0.000139	-
FN-6	0.4	0.0120	0.00739	0.0120	0.00739	-
FN-7	24.0	0.182	0.195	0.182	0.195	0.0850

Table 15: Tamarisk - Preliminary Data and Final Spreadsheet Determined Results

ID	Effective Porosity (%)	Permeability (md)				Liquid Permeability (md)
		Vertical	Horizontal	Vertical+	Horizontal+	Horizontal+
T-1	0.2	0.000127	0.000126	0.000127	0.000126	-
T-2	0.2	9.11 E-6	11.3 E-6	9.10 E-6	11.3 E-6	-
T-3	21.3	0.0406	0.156	0.0406	0.156	0.0610
T-4	21.7	0.0288	49.3	0.0288	49.3	7.51
T-5	0.2	71.9 E-6	54.6 E-6	71.9 E-6	54.6 E-6	-
T-6	0.3	0.000197	80.5 E-6	0.000197	80.5 E-6	-
T-7	1.0	0.0475	0.00604	0.0475	0.00604	-

+Permeability calculated using a spreadsheet program.

Table 16: Unknown Member - Preliminary Data and Final Spreadsheet Determined Results

ID	Effective Porosity (%)	Permeability (md)				Liquid Permeability (md)
		Vertical	Horizontal	Vertical+	Horizontal+	Horizontal+
UNM-1	26.8	0.0401	0.00953	0.0401	0.00953	0.00132
UNM-2	27.3	0.125	0.663	0.125	0.663	0.102
UNM-3	0.2	0.00298	0.00838	0.00298	0.00839	-

+Permeability calculated using a spreadsheet program.

5.2 Formation Factor

Formation Factor's (F_R) for the vertically oriented Culebra samples are reported in Table 17. Two- and four-pole values were determined, where possible. If sample lengths were inadequate, only two-pole data could be measured. When they are available, four-pole data are probably more appropriate (minimized end effects).

5.3 Pore Volume Compressibility

The results of the pore volume compressibility tests are provided in Tables 18 to 21. Graphs of volumetric strain versus stress, strain versus time, and stress versus time are provided for each pore volume compressibility test in Appendix E. Calibration data used for the pore volume compressibility tests are also included in Appendix E. Three compressibilities were determined for each sample. The first was determined from the initial hydrostatic loading (up to 500 psi). The second was determined during uniaxial strain loading, where both elastic and permanent deformation influence the compressibility. The third was determined during unloading, in uniaxial strain, where elastic response dominates.

Pore volume compressibility was calculated from the bulk compressibility and porosity. Porosity was remeasured prior to testing because a significant percentage of the samples contain gypsum. Test samples containing significant amounts of gypsum often loss or gain atmospheric moisture. Hence, the pore volume may change for these samples prior to pore volume compressibility testing. To alleviate this source of error, the porosity was remeasured immediately before the pore volume compressibility test. The porosity included in the compressibility tables is the remeasured value. ***Pore volume compressibility*** was not calculated for the majority of the anhydrite samples with extremely small porosities (less than 1%). To compute pore volume compressibility it is assumed that the bulk compressibility is significantly larger than the grain compressibility. For the low porosity anhydrite samples, this is not the case. In fact, the bulk compressibility is most likely to be close to the grain compressibility. Basic relationships approximate the pore volume compressibility as the bulk compressibility divided by the porosity. The resulting pore volume compressibility for a sample with a porosity of less than one percent will be excessively large. Possibly, for modelling purposes, the bulk compressibility may be a more realistic "compressibility" value to use for extremely low porosity rocks.

Note that miscellaneous Quality Assurance documents/records are provided in Appendix F.

Table 17: Formation Factor Measurements - Culebra Dolomite.

Sample ID	Depth (ft)	Formation Factor	
		2-Pole	4-Pole
C-1-V	741.35 - .60	47.71	42.98
C-2-V	741.80 - .90	60.3	N/A
C-3-V	742.00 - .20	76.04	63.57
C-4-V	743.00 - .20	57.99	53.03
C-5-V	743.30 - .50	85.24	77.61
C-6-V	744.25 - .50	128.71	112.73
C-7-V	745.15 - .40	139.73	111.51
C-8-V	746.00 - .15	136.58	124.47
C-9-V	746.75 - 747.00	155.22	139.85
C-10-V	747.35 - .60	138.15	121.08
C-11-V	747.75 - 748.00	134.52	119.87
C-12-V	748.30 - .55	146.02	134.28
C-13-V	749.10 - .30	17.56	N/A
C-14-V	750.00 - .20	218.79	N/A
C-15-V	756.25 - .40	126.77	N/A
C-16-V	756.70 - .80	392.18	N/A
C-17-V	756.50 - .60	45.16	N/A
C-18-V	757.00 - .20	148.93	150.74
C-19-V	759.10 - .35	83.91	82.33
C-20-V	759.80 - 760.00	40.08	38.14
C-21-V	760.20 - .40	72.89	66.59

Table 18: Magenta Pore Volume Compressibility Results

Sample ID	Porosity (%)	Hydrostatic Loading			Uniaxial Strain Loading			Uniaxial Strain Unloading		
		Stress Range (psi)	C_{bc} (10^{-6}/psi)	C_{pc} (10^{-6}/psi)	Stress Range (psi)	C_{bu} (10^{-7}/psi)	C_{pu} (10^{-6}/psi)	Stress Range (psi)	C_{bu} (10^{-7}/psi)	C_{pu} (10^{-6}/psi)
M-1A-V	10.06	148-378	1.6648	16.549	602-1452	2.9767	2.9589	1436-636	2.4721	2.4574
M-2-V	22.56	151-380	3.1402	12.286	515-1320	9.0133	3.5263	1319-616	4.7891	1.8737
M-3-V	18.58	146-400	1.5287	8.2277	650-1388	9.0616	4.8771	1377-634	4.8883	2.6309
M-4-V	11.49	153-404	0.8016	6.9765	705-1386	2.6683	2.3223	1346-654	1.8042	1.5702

C_{bc} - bulk compressibility under hydrostatic conditions.
C_{pc} - pore volume compressibility under hydrostatic conditions.
C_{bu} - bulk compressibility under uniaxial strain conditions.
C_{pu} - pore volume compressibility under uniaxial strain conditions.

Table 19: Forty-Niner Pore Volume Compressibility Results

Sample ID	Porosity (%)	Hydrostatic Loading			Uniaxial Strain Loading			Uniaxial Strain Unloading		
		Stress Range (psi)	C_{bc} (10^{-6}/psi)	C_{pc} (10^{-6}/psi)	Stress Range (psi)	C_{bu} (10^{-7}/psi)	C_{pu} (10^{-6}/psi)	Stress Range (psi)	C_{bu} (10^{-7}/psi)	C_{pu} (10^{-6}/psi)
FN-1-V	0.14	118-364	0.7878	Anhydrite	571-1432	0.6643	Anhydrite	1409-607	0.7340	Anhydrite
FN-2-V	0.10	103-344	0.8124	Anhydrite	567-1496	0.8428	Anhydrite	1360-618	1.1798	Anhydrite
FN-3-V	24.98	130-434	5.8804	23.5405	705-1455	28.3461	11.3475	1434-753	12.4239	4.9735
FN-4-V	16.19	103-354	3.7730	23.3043	539-1377	12.4734	7.7044	1322-674	6.7778	4.1864
FN-5-V	0.25	100-378	1.0206	Anhydrite	603-1457	1.0863	Anhydrite	1378-525	0.6562	Anhydrite
FN-6-V	3.39	113-392	1.2256	Anhydrite 36.1522	546-1385	3.0410	Anhydrite 8.97056	1294-757	1.8649	Anhydrite 5.5011
FN-7-V	25.43	125-426	5.8515	23.0100	633-1374	30.4394	11.9699	1279-594	11.0757	4.3554

C_{bc} - bulk compressibility under hydrostatic conditions.
C_{pc} - pore volume compressibility under hydrostatic conditions.
C_{bu} - bulk compressibility under uniaxial strain conditions.
C_{pu} - pore volume compressibility under uniaxial strain conditions.

TerraTek
University Research Park
420 Wakara Way • Salt Lake City, Utah 84108 •
Telephone (801) 584-2480
FAX (801) 584-2432

Table 20: Tamarisk Pore Volume Compressibility Results

Sample ID	Porosity (%)	Hydrostatic Loading			Uniaxial Strain Loading			Uniaxial Strain Unloading		
		Stress Range (psi)	C_{bc} (10^{-6}/psi)	C_{pc} (10^{-6}/psi)	Stress Range (psi)	C_{bu} (10^{-7}/psi)	C_{pu} (10^{-6}/psi)	Stress Range (psi)	C_{bu} (10^{-7}/psi)	C_{pu} (10^{-6}/psi)
T-1-V	0.48	129-430	0.7077	Anhydrite	634-1423	0.8834	Anhydrite	1384-704	0.6242	Anhydrite
T-2-V	0.17	153-443	0.8000	Anhydrite	761-1481	1.3393	Anhydrite	1449-813	1.0085	Anhydrite
T-3-V	22.08	148-501	5.1737	23.4316	775-1453	39.9941	18.1133	1404-836	12.3494	5.5930
T-4-V	22.70	174-451	7.7451	34.1194	802-1374	35.9465	15.8355	1380-862	13.8755	6.1126
T-5-V	0.21	150-472	0.5931	Anhydrite	744-1445	0.7671	Anhydrite	1426-817	0.8553	Anhydrite
T-6-V	1.58	192-450	0.6048	Anhydrite	752-1445	1.0718	Anhydrite	1410-712	0.6089	Anhydrite
T-7-V	4.79	175-449	2.3296	48.6347	785-1310	7.0515	14.7213	1400-814	2.5823	5.3910

C_{bc} - bulk compressibility under hydrostatic conditions.
C_{pc} - pore volume compressibility under hydrostatic conditions.
C_{bu} - bulk compressibility under uniaxial strain conditions.
C_{pu} - pore volume compressibility under uniaxial strain conditions.

Table 21: Un-Named Member Pore Volume Compressibility Results

Sample ID	Porosity (%)	Hydrostatic Loading			Uniaxial Strain Loading			Uniaxial Strain Unloading		
		Stress Range (psi)	C_{bc} (10^{-6}/psi)	C_{pc} (10^{-6}/psi)	Stress Range (psi)	C_{bu} (10^{-7}/psi)	C_{pu} (10^{-6}/psi)	Stress Range (psi)	C_{bu} (10^{-7}/psi)	C_{pu} (10^{-6}/psi)
UNM-1-V	27.93	249-553	4.7631	17.0537	840-1386	34.3991	12.3162	1385-876	15.2182	5.4487
UNM-2-V	28.71	173-553	7.3913	25.7447	937-1400	47.2820	16.4688	1329-804	15.5059	5.4009
UNM-3-V	1.38	123-426	1.2494	Anhydrite	818-1487	2.2966	Anhydrite	1433-789	1.9034	Anhydrite

C_{bc} - bulk compressibility under hydrostatic conditions.
C_{pc} - pore volume compressibility under hydrostatic conditions.
C_{bu} - bulk compressibility under uniaxial strain conditions.
C_{pu} - pore volume compressibility under uniaxial strain conditions.